Method to generate directly a broadband isolated attosecond pulse with stable pulse duration and high signal-to-noise ratio

Weiyi Hong, Peixiang Lu,* Pengfei Lan, Qianguang Li, Qingbin Zhang, Zhenyu Yang, and Xinbing Wang
Wuhan National Laboratory for Optoelectronics, Huazhong University of Science and Technology, Wuhan 430074, People's Republic of China

(Received 22 September 2008; revised manuscript received 19 October 2008; published 4 December 2008)

A method to generate a broadband isolated attosecond pulse with stable pulse duration and high signal-to-noise ratio is proposed. By adopting a few-cycle driving pulse combined with its second-harmonic field of which the polarization angle is $\pi/3$ with respect to the driving pulse, the short path is well selected and a smooth supercontinuum with the bandwidth of about 50 eV is observed, which leads to 100-as single attosecond pulse generation with high signal-to-noise ratio. More surprisingly, the intensity variation of the second-harmonic field can hardly affect the location and the bandwidth of the generated supercontinuum but only slightly reduce its phase-locking degree. For the intensity of the second-harmonic field higher than 10^{14} W/cm^2, a pure isolated attosecond pulse with duration of about 100 as can be generated by directly filtering out a supercontinuum from 85–125 eV, which facilitates the experimental implement of the isolated attosecond pulse generation.

DOI: 10.1103/PhysRevA.78.063407 PACS number(s): 33.80.Wz, 42.65.Ky, 42.65.Re

I. INTRODUCTION

High-order harmonic generation (HHG), which is a topic of great interest due to its potential application as a coherent soft-x-ray source [1] and the generation of attosecond pulses [2], has been rapidly developed. So far, the HHG is a unique way to produce attosecond pulses in experiments. The appearance of the attosecond pulses enable scientists to control and study the ultrafast dynamic processes with unprecedented resolution, and the attosecond pulse generation based on HHG has attracted a lot of attention. The HHG process can be well explained by the three-step model [3]: ionization, acceleration, and recombination. During the recombination, a photon with energy equal to the ionization potential plus the kinetic energy of the recombining electron is emitted. This process is repeated every half-cycle of the laser field, resulting in an attosecond pulse train with a periodicity of one-half an optical cycle. However, an isolated attosecond pulse is more useful in the pump-probe experiment. Much effort has been paid to extract a single attosecond pulse from the pulse train [2,4–10]. If the driving pulse contains only a few cycles, a supercontinuum appears at cutoff [2,4,5], which can be filtered out to produce a single attosecond pulse. Using a driving pulse with time-dependent ellipticity, i.e., the so-called polarization gate, the harmonics are emitted within a small part of the pulse, which supports the generation of a single attosecond pulse [6,7]. Recently, it has been proposed that an isolated attosecond pulse can be produced in a two-color multicycle pulse [8–10].

However, the typical bandwidth of the supercontinuum is less than 20 eV, then the duration of the shortest attosecond pulse is about 250 as, which limits its application. To further broaden the bandwidth of the supercontinuum and shorten the pulse duration, one should enlarge the difference between the highest and the second highest half-cycle photon energies, and a driving pulse containing nearly one optical cycle is needed, which has been achieved by Cavalieri *et al.* [11]. In their experiment, a sub-4 fs containing only a 1.5 optical cycle pulse has been successfully generated, and the bandwidth of the generated supercontinuum has been broadened to about 40 eV, which supports sub-100-as isolated pulse generation. But the requirement for such a driving pulse is rather stringent, which is still a big challenge for the current laser technology, and other approaches for broadening the supercontinuum are desired. By using a few-cycle laser pulse with the polarization gating technique [6,7], a broadband supercontinuum can be generated. After compensating the harmonic chirp, the duration of the isolated attosecond pulse is reduced to 130 as. It has also been theoretically reported that the broadband supercontinuum can be generated in a two-color pulse [12–15] and this probability has been experimentally proved recently [16].

Both classical [3] and quantum calculations [17] show two dominant electron trajectories contributing to the HHG, namely, the so-called long and short trajectories, characterized by the traveling times of the electrons in the continuum. Since the harmonics from the long and short paths have different emission times, for the supercontinuum generation based on HHG, the interference of the harmonics from long and short paths leads to a modulation structure in the continuous spectrum. In every half-cycle of the laser pulse, there are two peaks in the generated attosecond pulses, which originate from the long and short paths, respectively. Then the application of the attosecond pulses will be limited. Therefore, the quantum path control plays an important role for the manipulation of HHG and isolated attosecond pulse generation, and many techniques have been proposed to the quantum path selection. Macroscopically, the short quantum path can be selected via carefully adjusting the phase-matching condition [18] or spatial filtering [19]. In the single atom response, both a collinearly polarized two-color field [20] and an orthogonally polarized two-color field [21] can be applied to selecting a quantum path, resulting in the gen-

*Corresponding author: lupeixiang@mail.hust.edu.cn

eration of a regular attosecond pulse train or a pure isolated attosecond pulse. For the broadband isolated pulse generation in the collinearly polarized two-color field, the location and the bandwidth of the supercontinuum are sensitively dependent on the relative phase and intensities of the two-color field. Then the condition of the quantum path selection is also rather stringent, and the intensity variation of the second-harmonic field may reduce the signal-to-noise ratio of the generated single attosecond pulse, which would bring some difficulties in the experimental realization. In this paper, we propose a method to generate stably a broadband isolated attosecond pulse. In our method, a few-cycle fundamental pulse in combination with its second-harmonic field of which the polarization angle is $\pi/3$ is adopted. A supercontinuum with the bandwidth of about 50 eV is observed and the short path is well selected, resulting in a 100-as isolated attosecond pulse with high signal-to-noise ratio. It is found that the variation of the intensity of the second-harmonic field does not change the location and the bandwidth of the supercontinuum. More surprisingly, if the intensity of the second-harmonic field is significantly high, its variation only slightly affects the phase-locking degree of the supercontinuum, which implies that a broadband isolated attosecond pulse with high signal-to-noise ratio can be generated in different intensities of the second-harmonic field.

II. RESULT AND DISCUSSION

In this paper, we consider the interaction between the atom and the two-color laser pulse in the single active electron approximation and numerically solve the two-dimensional time-dependent Schrödinger equation in terms of the split-operator method [22]. In our simulation, we use a soft-core potential model $V(x,y)=-1/(\alpha+x^2+y^2)^{1/2}$ and choose the softening parameter α to be 0.07 corresponding to the ionization energy of 24.6 eV for the ground state of the helium atom. The two-color laser pulse is synthesized by a 5 fs, 800 nm fundamental field and its second-harmonic field. The intensities of these two fields are chosen to be 6×10^{14} W/cm^2 and 3×10^{14} W/cm^2, respectively. The electric field of the synthesized two-color pulse is expressed by

$$\vec{E}(t) = f(t)\{[E_\omega \cos(\omega t) + E_{2\omega}\cos(\theta)\cos(2\omega t + \phi)]\hat{\mathbf{x}} + E_{2\omega}\sin(\theta)\cos(2\omega t + \phi)\hat{\mathbf{y}}\}.$$

Here E_ω and $E_{2\omega}$ are the amplitudes of the fundamental and second-harmonic fields, respectively. $f(t)=\exp[-2\ln(2)t^2/(\tau)^2]$ presents the profile of the two-color pulse and $\tau=5$ fs is the pulse duration full width at half-maximum (FWHM). ϕ is the relative phase and is chosen to be 0.5π. $\theta=\pi/3$ is the polarization angle between the fundamental and the second-harmonic fields. The three-dimensional (3D) plot of the electric field is shown in Fig. 1.

Figures 2(a) and 2(b) show the harmonic spectrum in the two-color synthesized pulse of the fundamental pulse and its second-harmonic field (red thick line). The parameters are the same as those in Fig. 1. For comparison, the harmonic spectra in the fundamental pulse (black dashed line), its second-harmonic field (orange dashed line) alone, and the perpendicularly polarized two-color field (green thin line) are also presented in Fig. 2(a) and the high-energy part of the harmonic spectrum in the paralleled polarized two-color field (blue dashed line) are presented in Fig. 2(b). Note that the intensity of harmonic spectrum generated in the two-color pulse is obtained by summing up the intensity of the x component and the y component of the harmonics. For the one-color cases, the spectrum cutoffs of the 800 nm/5 fs pulse and the 400 nm/5 fs pulse are at 36th and 92nd harmonics, corresponding to 56 eV and 143 eV, respectively. For the two-color case with the polarization angle of $\pi/3$, the spectrum cutoff is at the 85th harmonic, corresponding to 132 eV. One can clearly see that the harmonics above the

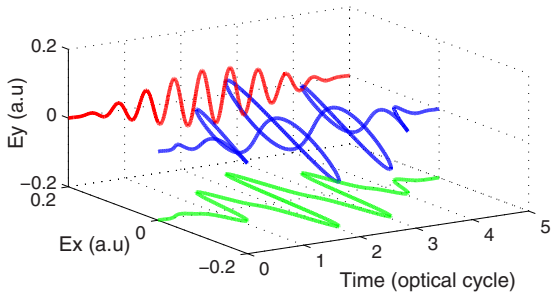

FIG. 1. (Color online) The 3D plot of the two-color field. The laser parameters are 800 nm/5 fs, with the intensity of 6×10^{14} W/cm^2 and 400 nm/5 fs, with the intensity of 3×10^{14} W/cm^2. The polarization angle between these two fields is $\pi/3$.

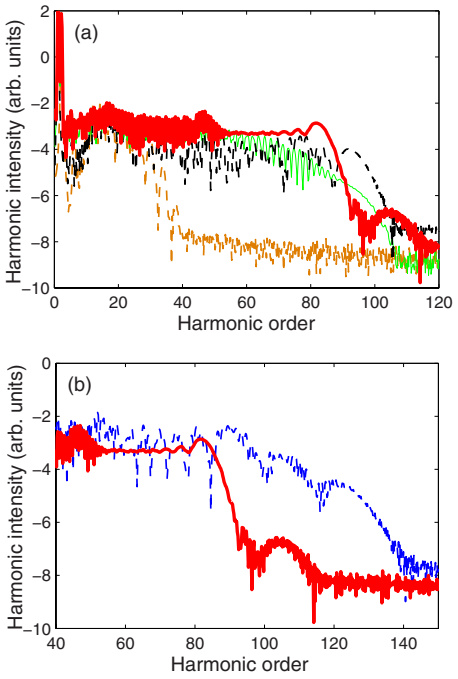

FIG. 2. (Color online) (a) The harmonic spectra in the two-color field with the polarization angle of $\pi/3$ (red thick line) and $\pi/2$ (green thin line), in the single color 800 nm/5 fs field (black dashed line) and in the single color 400 nm/5 fs field (orange dashed line). (b) High-energy part of the harmonic spectra for the cases of $\pi/3$ (red thick line) and parallel polarization (blue dashed line). Other parameters are the same as in Fig. 1.

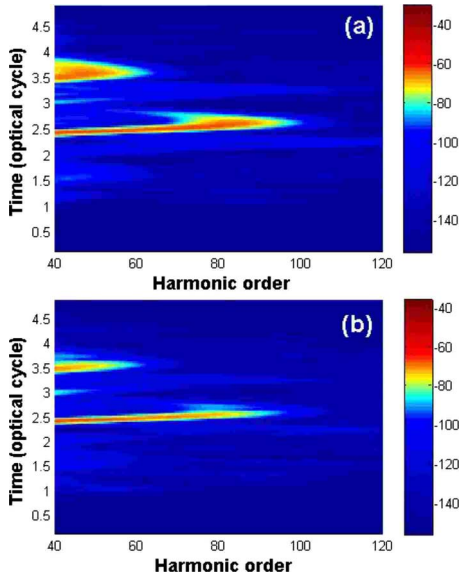

FIG. 3. (Color online) Time-frequency distribution of (a) x component and (b) y component of HHG in the two-color field with the polarization angle of $\pi/3$. The parameters are the same as in Fig. 1.

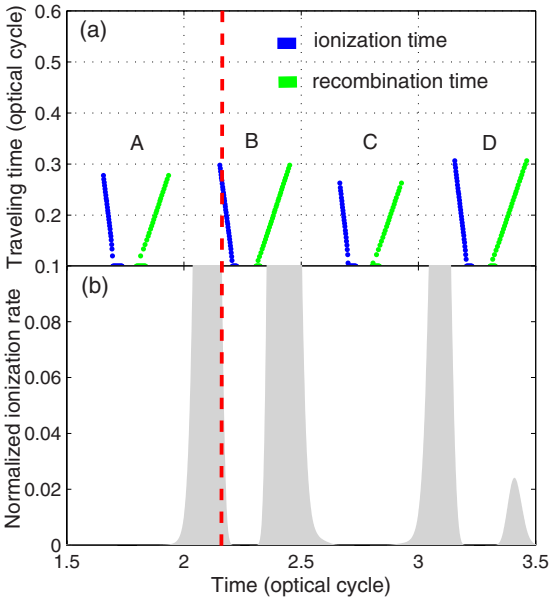

FIG. 4. (Color online) (a) The traveling times as a function of the ionization (blue dots) and recombination times (green dots) and (b) the tunnel ionization rate calculated by the Ammosov-Delone-Krainov (ADK) model. The parameters are the same as in Fig. 1.

53rd (82 eV) harmonic become continuous, leading to a supercontinuum with the bandwidth of 50 eV. Moreover, the harmonic intensity is about one order higher than that in the 800 nm/5 fs pulse alone. For the perpendicularly polarized case, the cutoff is higher than that of the $\pi/3$ case, but the bandwidth of the supercontinuum is only 24 eV. It is clear that the harmonic yield decreases rapidly as the harmonic order increases near the cutoff region and the intensity of the supercontinuum is at least 3 orders lower than that of the $\pi/3$ case. One can clearly see from Fig. 2(b) that the cutoff of the harmonic spectrum in a paralleled polarized two-color field is higher than that of the $\pi/3$ case, but the high-energy part of the spectrum shows some interference and a multiplateau structure.

A deeper insight is obtained by investigating the emission time of the harmonics for the case of the two-color field with the polarization angle of $\pi/3$ in terms of the time-frequency analysis method [24], as shown in Fig. 3. Figures 3(a) and 3(b) are the time-frequency distribution of the x component and y component of HHG in the two-color field, respectively. There are two peaks contributing to the harmonics for both components. The first peak is at about 2.5 T (optical cycle) and the second one is at about 3.5 T. For the x component, the maximum harmonic order of the first peak is 85 (132 eV) and that of the second peak is 53 (82 eV). For the y component, the maximum harmonic order of the first peak is 75 (116 eV) and that of the second peak is 50 (78 eV). It is clear that only one path contributes to the HHG of the first peak, i.e., the harmonics of the first peak are phase locked, for both components. Taking into account all of these results, we can conclude that the harmonics higher than 82 eV are almost locked in phase and emit once, i.e., become a supercontinuum; for the harmonics below 82 eV, the interference of the two peaks leads to the irregular structure in the spectrum, which is shown in Fig. 2.

To more clearly understand the time-frequency properties of the HHG shown in Fig. 2 and Fig. 3, we investigate the HHG process in the two-color field by the semiclassical three-step model [3]. As mentioned above, for each harmonic, the long trajectory has the earlier ionization but later recombination time and the short one has the later ionization but earlier recombination time. Therefore, the traveling time (the difference between the ionization and recombination times) of the long trajectory is longer than that of the short trajectory. Typically, the traveling time of the long trajectory is longer than 0.65 T while that of the short trajectory is shorter than 0.65 T. This critical value between the traveling times of long and short trajectories is slightly affected by the second-harmonic field, then this distinction is still meaningful for the $\omega+2\omega$ two-color scheme (T refers to the optical cycle of the fundamental field). Figure 4 shows the electron dynamics of the HHG process in the two-color field; the parameters are the same as those in Fig. 1. Figure 4(a) is the traveling time as the function of the ionization (blue dots) and recombination times (green dots) and Fig. 4(b) is the tunnel ionization rate calculated by the Ammosov-Delone-Krainov (ADK) model (gray filled curve) [23]. As shown in Fig. 4(a), there are four couples of the ionization and recombination times within the duration of the laser pulse (marked as A, B, C, and D). The maximum traveling time is about 0.3 T, which indicates that only the short trajectories contribute to the HHG. In our simulation, the intensity of the laser field is much lower than the saturation intensity of the helium atom. According to the three-step model, the harmonic efficiency is mainly determined by the first step, i.e., the ionization rate. As shown in Fig. 4(b), the ionization rate near the ionization times of A and C are much lower than that of B and D, and then the contributions of A and C to the HHG are ignorable. The recombination times of B (as the red dashed line indicates) and D are near 2.5 T and 3.5 T, which means that the harmonics are emitted near these two times.

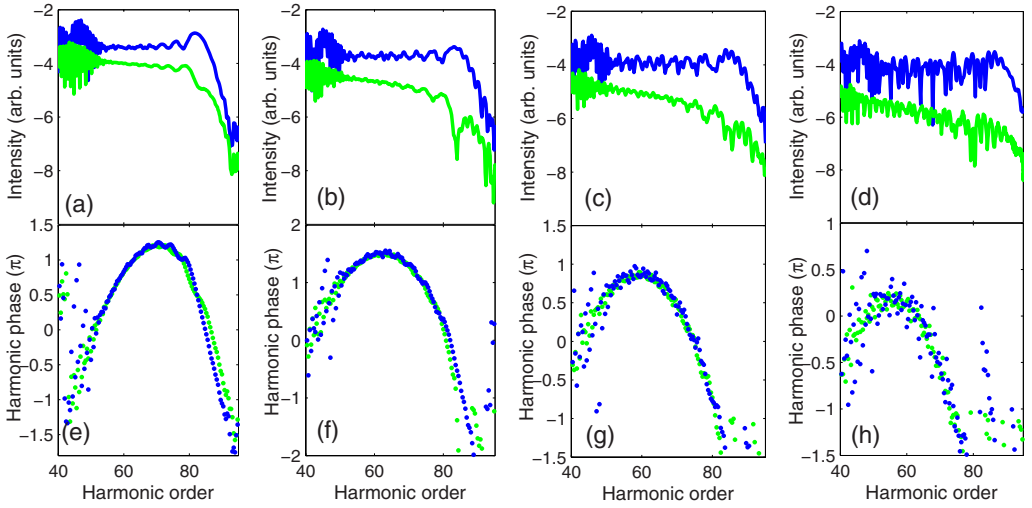

FIG. 5. (Color online) (a)–(d) The harmonic spectra with four different intensities of the second-harmonic field: 3×10^{14} W/cm^2, 1.5×10^{14} W/cm^2, 1×10^{14} W/cm^2, and 5×10^{13} W/cm^2, respectively. (e)–(h) The harmonic phases for the cases of four corresponding intensities; blue and green dots present the harmonic phases of the x and y components of the HHG, respectively. Other parameters are the same as those in Fig. 1.

All of these results are confirmed by the quantum calculation shown in Fig. 2 and Fig. 3.

Finally, we investigate the HHG processes in the two-color field with different intensities of the second-harmonic field. Figures 5(a)–5(d) are the harmonic spectra for the cases of four different intensities: 3×10^{14} W/cm^2, 1.5×10^{14} W/cm^2, 1×10^{14} W/cm^2, and 5×10^{13} W/cm^2, respectively. Other parameters are the same as those in Fig. 1. The blue and green lines present the spectra of the x component and y component, respectively. As the intensity of the second-harmonic field decreases, the harmonic yield of the y component decreases rapidly, especially for the harmonics near the cutoff, which leads to a slope in the spectrum. For the spectra of the x component, one can clearly see that the harmonic cutoffs are almost the same as the intensity of the second-harmonic field decreases. For the cases of 1.5×10^{14} W/cm^2 and 1×10^{14} W/cm^2, the harmonics above 53rd are still continuous, although there are some slight modulations on the supercontinuum. For the case of 5×10^{13} W/cm^2, the harmonic spectrum becomes irregular except for the cutoff region.

In addition, we also present the harmonic phases for the cases of four corresponding intensities, which are shown in Figs. 5(e)–5(g); blue and green dots present the harmonic phases of the x and y components of the HHG, respectively. For the case of 3×10^{14} W/cm^2, there are clear nearly, parabolic profiles across the supercontinuum (from the 53rd to 85th harmonic), both for the x and y components, which implies that the harmonic phases are almost linearly chirped, i.e., the harmonics are locked in phase. When the intensity of the second-harmonic field decreases to 1.5×10^{14} W/cm^2 and 1×10^{14} W/cm^2, the definition of the harmonic phase profile decreases to some extent, which means that the phase-locking degree decreases. For the case of 5×10^{13} W/cm^2, the harmonic phases become somewhat chaotic.

Further, we consider the isolated attosecond pulse generation for the cases of four different intensities of the second-harmonic field. Here the harmonics for 55th to 80th are selected. The bandwidth of the selected harmonics is about 40 eV, corresponding to an isolated attosecond pulse with the duration of about 95 as in the Fourier-transform limit. The temporal profile of the attosecond pulse can be obtained by performing the inverse Fourier transformation in the selected spectrum region. In order to clearly show the polarization characteristics of the generated attosecond pulses, we first present the three-dimensional (3D) plots of the electric fields of the attosecond pulses for the cases of four different intensities of the second-harmonic field, which are shown in Figs. 6(a)–6(d). The parameters are the same as those in Fig. 5. For the case of 3×10^{14} W/cm^2, there is one pure attosecond pulse both for the x and y components. As the intensity of the second-harmonic field decreases, the magnitude of the electric field of the y component decreases much faster than that of the x component, which implies that the decrease of the second-harmonic field will change the polarization of the generated attosecond pulses. For the case of 1×10^{14} W/cm^2, one can see there are some very small satellite pulses after the main pulse, and for the case of 5×10^{13} W/cm^2, the magnitudes of the satellite pulses increase.

After summing up the intensities of the x and y components, the temporal envelopes of the generated attosecond pulses are obtained, which are shown in Fig. 7. The temporal envelopes of the attosecond pulses for the cases of 3×10^{14} W/cm^2, 1.5×10^{14} W/cm^2, 1×10^{14} W/cm^2, and 5×10^{13} W/cm^2 are shown by the blue, orange, green, and black lines, respectively. For the cases of 3×10^{14} W/cm^2, 1.5×10^{14} W/cm^2, and 1×10^{14} W/cm^2, pure isolated attosecond pulses are observed. Concretely, the maximum energies of the satellite pulses are only about 1.5%, 3%, and 5% of the main pulses for these three cases, respectively. The durations of the main pulses for these three cases are about 98 as, 102 as, and 107 as, which are very close to the Fourier-transform limit. The inset is the detail of the tempo-

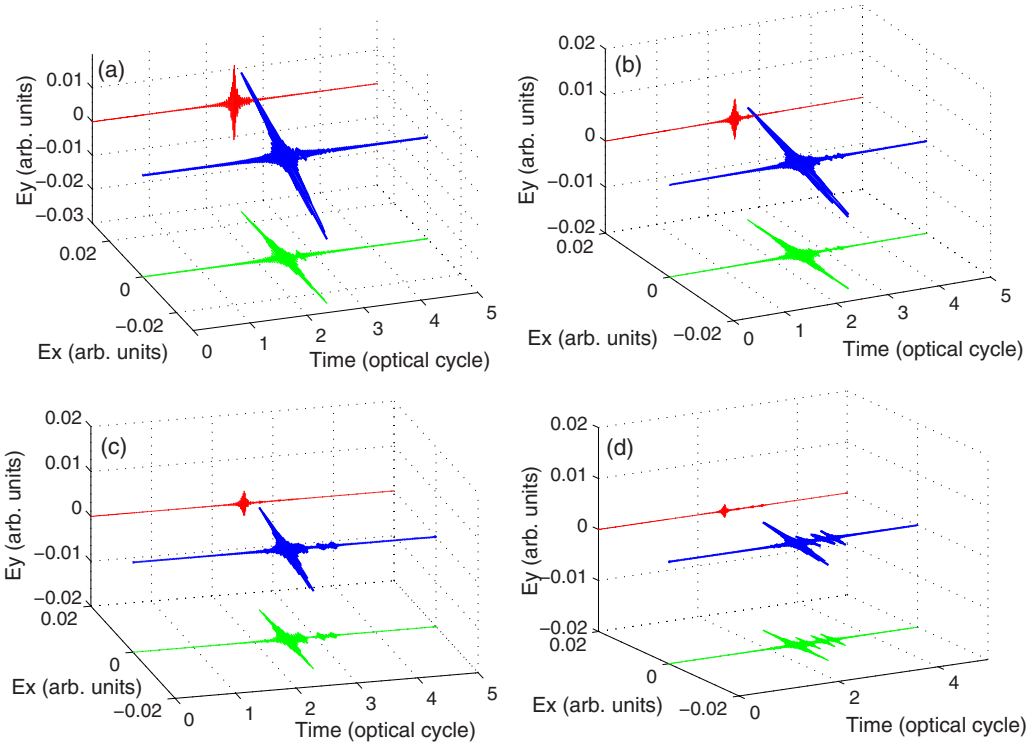

FIG. 6. (Color online) (a)–(d) The 3D plots of the electric fields of the attosecond pulses for the four intensities of the second-harmonic field: 3×10^{14} W/cm^2, 1.5×10^{14} W/cm^2, 1×10^{14} W/cm^2, and 5×10^{13} W/cm^2, respectively. Other parameters are the same as those in Fig. 1.

ral envelope of the generated attosecond pulses for the case of 5×10^{13} W/cm^2. There are three satellite pulses with 20% energy of the main pulse. Note that the central wavelength of the selected harmonics is at about 105 eV, and the generated isolated pulse only contains 2.5 optical cycles. Analogous to the few-cycle infrared pulse, such a few-cycle isolated attosecond pulse may be a powerful tool to study and control the electronic dynamics which are induced by the electric field rather than the intensity profile in the extreme ultraviolet region.

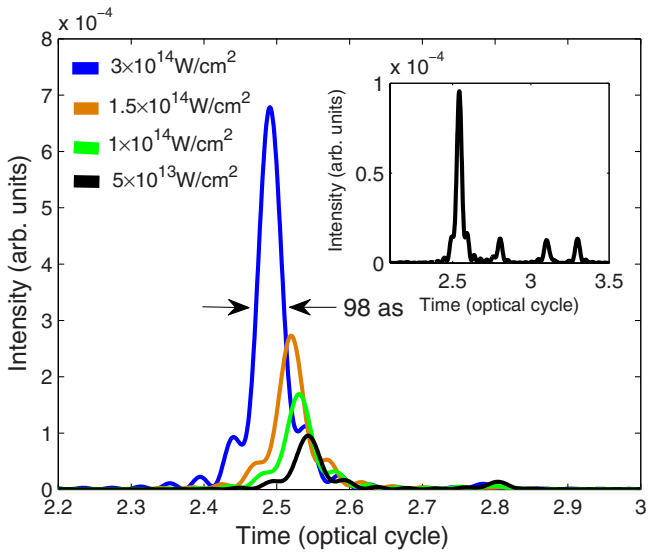

FIG. 7. (Color online) The temporal envelopes of the generated attosecond pulses in the two-color field, the cases of 3×10^{14} W/cm^2, 1.5×10^{14} W/cm^2, 1×10^{14} W/cm^2, and 5×10^{13} W/cm^2 are shown by the blue, orange, green, and black lines, respectively. The inset is the detail of the temporal envelope of the generated attosecond pulses for the case of 5×10^{13} W/cm^2.

III. CONCLUSION

In conclusion, we propose a method to generate a broadband isolated attosecond pulse with stable pulse duration and high signal-to-noise ratio. In our method, a few-cycle fundamental pulse in combination with its second-harmonic field of which the polarization angle is $\pi/3$ is adopted. A supercontinuum with the bandwidth of about 50 eV is observed and the short path is well selected, resulting in a 100-as isolated attosecond pulse with high signal-to-noise ratio. For different intensities of the second-harmonic field, the location and the bandwidth of the generated supercontinuum almost keep stable, and the phase-locking degree slightly decreases as the intensities of the second-harmonic field decreases. If this intensity is higher than 1×10^{14} W/cm^2, a pure isolated attosecond pulse with the duration of about 100 as can be generated by directly filtering out a supercontinuum from 85–125 eV. These fascinating properties have many advantages which facilitate the experimental implement for the broadband isolated attosecond pulse generation. Experimentally, the 5-fs phase-stabilized few-cycle pulse can

be generated by the cascade filamentation compression technique, and the second-harmonic field can be obtained from a BBO crystal. From our simulation, the HHG spectrum is not sensitive to the pulse duration of the second-harmonic field, even if the pulse duration is longer than 15 fs. However, the relative phase should be accurately controlled. From our simulation we found that the fluctuation range of the relative phase should be controlled within $\pm 0.1\pi$, otherwise some modulations will appear in the continuous part of the spectrum and the signal-to-noise ratio of the produced attosecond pulse will decrease. Control of the relative phase with such accuracy can be experimentally achieved by a piezoelectric translator [25].

ACKNOWLEDGMENTS

This work was supported by the National Natural Science Foundation of China under Grants No. 10574050, and No. 10774054, No. 10734080 and the National Basic Research Program of China under Grant No. 2006CB806006. This work was partially supported by the State Key Laboratory of Precision Spectroscopy of Huadong Normal University.

[1] Z. Chang, A. Rundquist, H. Wang, M. M. Murnane, and H. C. Kapteyn, Phys. Rev. Lett. **79**, 2967 (1997).
[2] R. Kienberger, E. Goulielmakis, M. Uiberacker, A. Baltuska, V. Yakovlev, F. Bammer, A. Scrinzi, Th. Westerwalbesloh, U. Kleineberg, U. Heinzmann, M. Drescher, and F. Krausz, Nature (London) **427**, 817 (2004).
[3] P. B. Corkum, Phys. Rev. Lett. **71**, 1994 (1993).
[4] M. Hentschel, R. Kienerger, C. Spilmann, G. A. Reider, N. Milosevic, T. Brabec, P. Corkum, U. Heinzmann, M. Drescher, and F. Krausz, Nature (London) **414**, 509 (2001).
[5] I. P. Christov, M. M. Murnane, and H. C. Kapteyn, Phys. Rev. Lett. **78**, 1251 (1997).
[6] Z. Chang, Phys. Rev. A **71**, 023813 (2005).
[7] G. Sansone, E. Benedetti, F. Calegari, C. Vozzi, L. Avaldi, R. Flammini, L. Poletto, P. Villoresi, C. Altucci, R. Velotta, S. Stagira, S. De Silvestri, and M. Nisoli, Science **314**, 443 (2006).
[8] T. Pfeifer, L. Gallmann, M. J. Abel, D. M. Neumark, and S. R. Leone, Opt. Lett. **31**, 975 (2006).
[9] H. Merdji, T. Auguste, W. Boutu, J. P. Caumes, B. Carre, T. Pfeifer, A. Jullien, D. M. Neumark, and S. R. Leone, Opt. Lett. **32**, 3134 (2007).
[10] W. Cao, P. Lu, P. Lan, X. Wang, and G. Yang, Opt. Express **15**, 530 (2007).
[11] A. L. Cavalieri, E. Goulielmakis, B. Horvath, W. Helml, M. Schultze, M. Fieß, V. Pervak, L. Veisz, V. S. Yakovlev, M. Uiberacker, A. Apolonski, F. Krausz, and R. Kienberger, New J. Phys. **9**, 242 (2007).
[12] P. Lan, P. Lu, W. Cao, Y. Li, and X. Wang, Phys. Rev. A **76**, 011402(R) (2007).
[13] P. Lan, P. Lu, W. Cao, Y. Li, and X. Wang, Phys. Rev. A **76**, 051801(R) (2007).
[14] W. Hong, P. Lu, P. Lan, Z. Yang, Y. Li, and Q. Liao, Phys. Rev. A **77**, 033410 (2008).
[15] Q. Zhang, P. Lu, P. Lan, W. Hong, and Z. Yang, Opt. Express **16**, 9795 (2008).
[16] Y. Zheng, Z. Zeng, X. Li, X. Chen, P. Liu, H. Xiong, H. Lu, S. Zhao, P. Wei, L. Zhang, X. Wang, J. Liu, Y. Cheng, R. Li, and Z. Xu, Opt. Lett. **33**, 234 (2008).
[17] M. Lewenstein, Ph. Balcou, M. Yu. Ivanov, A. L'Huillier, and P. B. Corkum, Phys. Rev. A **49**, 2117 (1994).
[18] P. Antoine, A. L'Huillier, and M. Lewenstein, Phys. Rev. Lett. **77**, 1234 (1996).
[19] R. López-Martens, K. Varjú, P. Johnsson, J. Mauritsson, Y. Mairesse, P. Salières, M. B. Gaarde, K. J. Schafer, A. Persson, S. Svanberg, C. G. Wahlström, and A. L'Huillier, Phys. Rev. Lett. **94**, 033001 (2005).
[20] W. Cao, P. Lu, P. Lan, W. Hong, and X. Wang, J. Phys. B **40**, 869 (2007).
[21] C. M. Kim, I. J. Kim, and C. H. Nam, Phys. Rev. A **72**, 033817 (2005).
[22] M. D. Feit, J. A. Fleck, Jr., and A. Steiger, J. Comput. Phys. **47**, 412 (1982).
[23] M. V. Ammosov, N. B. Delone, and V. P. Krainov, Sov. Phys. JETP **64**, 1191 (1986).
[24] P. Antoine, B. Piraux, and A. Maquet, Phys. Rev. A **51**, R1750 (1995).
[25] H. Mashiko, S. Gilbertson, C. Li, S. D. Khan, M. M. Shakya, E. Moon, and Z. Chang, Phys. Rev. Lett. **100**, 103906 (2008).